

Linear gradient analysis of kinetic temperature through geostatistical approach

Deepak Kumar¹  · Sulochana Shekhar²

Received: 13 July 2016 / Accepted: 14 July 2016 / Published online: 2 August 2016
© Springer International Publishing Switzerland 2016

Abstract Urban sprawl is one of the main problems which conceives the concepts of the thermal gradient. The use of thermal remote sensing methods and availability of computer hardware had made possible to quantify the amount unprecedented increase to provide inputs to planners towards computation of urban growth. Thermal remote sensing technology along with geostatistics has shown its great capabilities in solving many of this computational issues. The intended to monitor potential vagaries that may occur raising issues concerning thermal divergence, particularly in the urban areas and agriculture areas. Kinetic temperature worked as absolute parameters to study the linear gradient analysis distribution to analyse the variability in the spatial domain. The zonal or ortho-directional thermal gradient techniques were devised in the geostatistical techniques domain to estimate the gradient in all directions. Partially the works covered the aspects of thermal image processing along with characterization of spatial (x, y) and thermal (t) trends. The correlation among surface temperature values within urban–rural areas were also attempted. The results apparently indicated the increasing thermal gradient configuration along urbanization areas and vice versa. The work validated the approach

of combination of zonal thermal gradient analysis as a reliable tool to monitor the thermal dynamics and also discoursed the role of surface kinetic temperature towards major research approaches functional to the urban studies.

Keywords Linear · Thermal · Geostatistics · Spatial · Gradient · Kinetic

Introduction

The 21st century society is often called information society. A large number of decisions in our daily life made by governmental, non-governmental organizations and by individuals are based on geospatial information. Nevertheless, especially in developing countries, we can observe a lack of spatial information. Rapid advancement and extension of urban development in countries like India is enduring to be one of the key issues affecting the physical dimensions of cities leading to several landscape variations due to upcoming buildings, roads, and other infrastructure replacing all the open land and vegetation cover. There is no sign of decelerating down of this progression and it is the most powerful and visible anthropogenic strength which has brought vital changes in urban land cover and landscape pattern of the country. All the surfaces that were permeable and moist become impermeable and dry. These changes the urban regions into the warmer region than their rural surroundings, forming an “island” of higher temperatures (Yuan and Bauer 2007). Urban growth leads to the change of land use and land cover in many areas around the world, especially in developing countries (Belal and Moghanm 2011). Remote sensing data are very useful to the several studies due to its competency to provide a synoptic view, repetitive coverage along with the real-time

✉ Deepak Kumar
deepakdeo2003@gmail.com

Sulochana Shekhar
sulogis@gmail.com

¹ Amity Institute of Geoinformatics and Remote Sensing (AIGIRS), Amity University, Room No-05, Ground Floor, J-1 Block, Amity University Campus, Sector 125, Gautam Buddha Nagar, Noida, Uttar Pradesh 201303, India

² Department of Geography, School of Earth Sciences, Central University of Karnataka, Aland Road, Kadaganchi, Kalaburagi (Gulbarga Dist.), Karnataka 585 367, India

data acquisition. The digital data in the form of satellite imageries, therefore, enable us accurately compute various land cover/land use categories and helps in maintaining the spatial data infrastructure which is very crucial for monitoring urban studies in multiple aspects. Land use land cover (LULC) change contributes decision makers to ensure sustainable development and to understand the dynamics of our changing environment (Iqbal and Khan 2014). LULC classification of a satellite image is one of the prerequisites and plays an indispensable role in many land use inventories and environmental modeling. Many studies viz., forest inventories, hydrology and biodiversity studies, etc., are in demand to account the dynamics of land use and phenology of vegetation. Multi-temporal land use classification accounts the phenology of vegetation and land use dynamics of the study area (Kanyakumari and Neelamsetti 2015). LULC change detection helps the policy makers to understand the environmental change dynamics to ensure sustainable development. Hence, LULC feature identification has emerged as an important research aspect and thus, a proper and accurate methodology for LULC classification is the need of time (Sinha et al. 2015).

Kinetic temperature (KT), acts an important indicator in the study of energy balance models on the ground and the greenhouse effect of surface interactions in regional and global scale. KT is derived from thermal infrared data supplied by band 6 of the Enhanced Thematic Mapper plus (ETM+) sensor onboard the Landsat 7 satellite (Sun et al. 2014). Various algorithms like single-channel methods, split-window technique and multi-angle methods have been developed to retrieve LST from at-sensor and auxiliary data. The present study discourses the utility of thermal remote sensing in multiple aspects. The thermal satellite imagery were processed to obtain the at-surface kinetic temperature for carrying major portion of the research. These inclusive values are managed with the minimum input to perform the further analyses with the geostatistical analysis, which cannot be deliberated by man-made ability. The main objective of this study was to investigate the extent and divergence of at-surface kinetic temperature in urban as well rural (rural–urban fringe) occurred due to the urban sprawl and its impact on joint land use changes integrating remote sensing and GIS.

This work also study and analyze the variance of gradient on ortho-directional or zonal extents due to land cover change through the utilization of extracted at-surface kinetic temperature. It basically also focused on the techniques to extract quantitative information through thermal data in a specific direction with respect to a reference point. Rationally the works covers the aspects of thermal image processing, characterization of spatial (x, y) and thermal (t) trends.

The following facets deliberated to achieve the main objectives (1) detect the extent of urban and rural extent, (2) computing at-surface kinetic temperature from satellite imagery for the study area, (3) distributing the obtained result from imagery into sectors or ortho-directions, (4) visualizing the boundary of the urban core limits and its rural extents, (5) generating random sample points in each of the sectoral limits of urban core as well as in rural extent, (6) analyzing the degree of similarity vs dissimilarity in both the limits of urban land cover and existing land use, (7) investigating the structure and patterns of variability, (8) examining the impact of urbanization on the land cover/land use changes, and (9) computing the gradient along the ortho-directional sectors.

Materials and methods

Study area

The current study has been carried out at Kalaburagi city (formerly known as Gulbarga City) located at the northern part of the Karnataka State in India. It is situated in Deccan Plateau and the general average elevation is 454 m above mean sea level. Black soil is predominant soil type in the district ("<http://www.gulbarga.nic.in>", 2015) including city locality. Until very recently, it was a sleepy town having very limited outskirts. It lies in the extends between 76°0.04' and 77°0.42' east longitude, and 17°0.12' and 17°0.46' north latitude, covering an area of 81–365 km² from the urban core to outskirts. The city is undergoing rapid changes in terms of population growth as well as in the degree of urbanization. The city consists of three main seasons: the summer spanning from late February to mid-June (38–44 °C), followed by the south-west monsoon spanning from the late June to late September with heavy rainfall up to 750 mm (27–37 °C), and lastly, it has dry winter weather until mid-January (11–26 °C) ("<http://www.gulbarga.nic.in>", 2015). The main purpose behind the selection of the said study area was the author familiarity and accessibility of resources. The below Fig. 1 describes the location of the study area in detail.

Datasets and software's

A Landsat 7 ETM+ image acquired on December 4th, 2000 has served as the primary data source for driving the whole research work including KT derivations. Different geospatial software's and tools covering ERDAS 9.2, Arc Desktop 10.x, and ENVI 4.7 were used. The ERDAS software was used for image processing and calibration purposes, Arc Desktop were utilised for mapping and layout purposes. Likewise, the ENVI was utilized for the major of the work

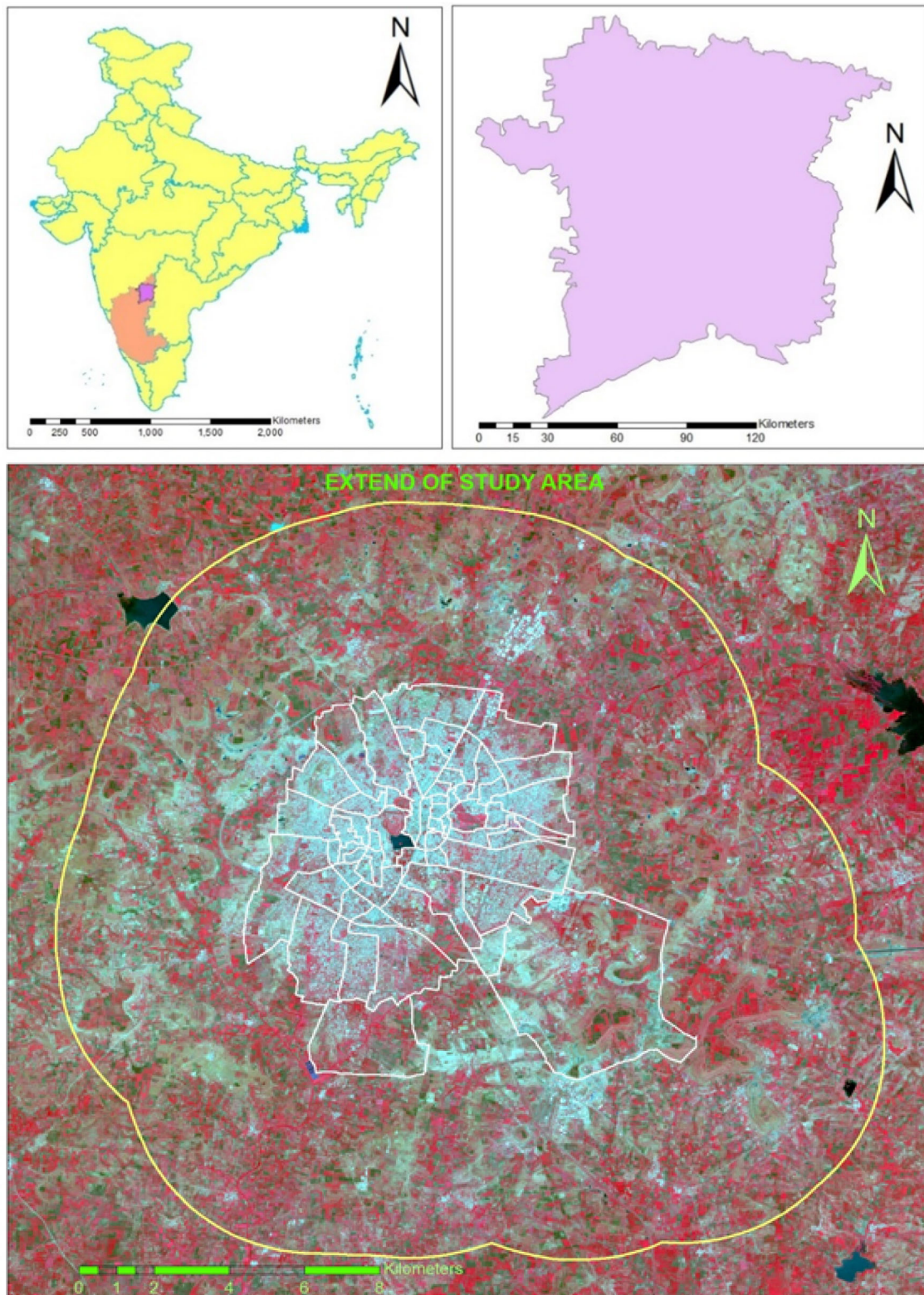


Fig. 1 Study area

including thermal band calibrations and thermal image processing including SRT derivation purposes. Table 1 describes the characteristics of ETM+ sensors along with

band properties. The present study involved the collection of topographic sheets from Survey of India and city map from relevant authorities. The required satellite imagery for the

Table 1 Characteristics of enhanced thematic mapper plus (ETM+) bands

Band	Spatial resolution (m)	Lower limit (μm)	Upper limit (μm)	Bandwidth (nm)	Bits per pixel	Gain	Offset
1	28.50	0.45	0.52	70	8	0.786274521	-6.1999998
2	28.50	0.53	0.61	80	8	0.817254878	-6.0000000
3	28.50	0.63	0.69	60	8	0.639607867	-4.5000000
4	28.50	0.75	0.90	150	8	0.939215686	-4.5000000
5	28.50	1.55	1.75	200	8	0.128470589	-1.0000000
6	57.00	10.40	12.50	2100	8	0.066823533	0.0000000
7	28.50	2.10	2.35	250	8	0.044243138	-0.3499999
8	14.25	0.52	0.90	380	8	0.786274521	-6.1999998

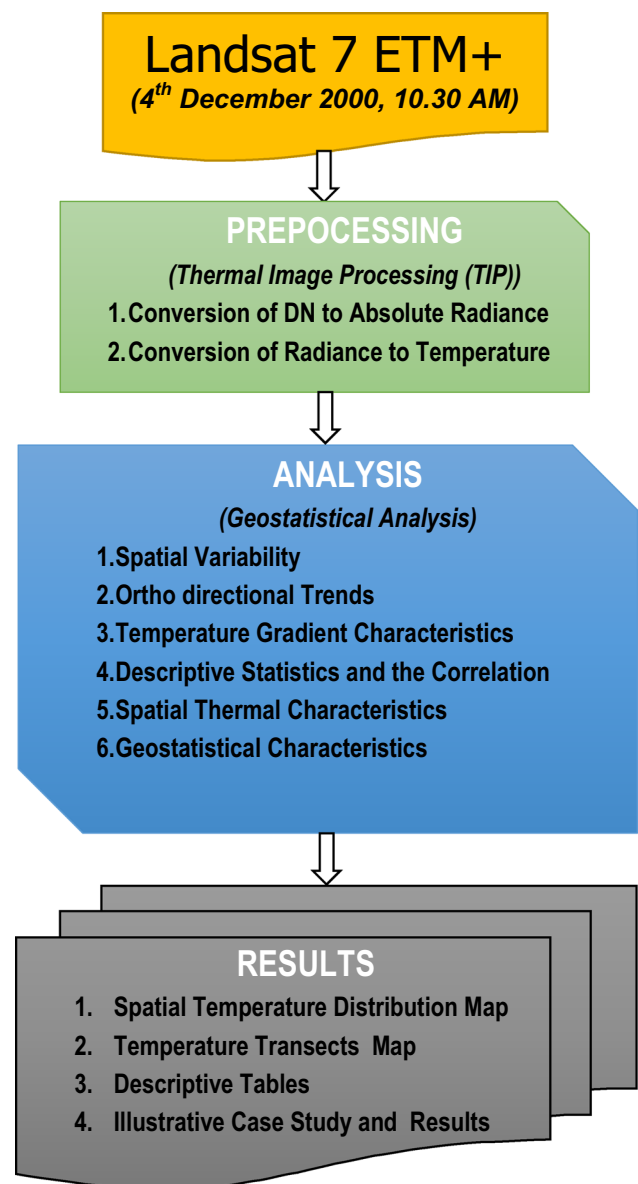
study area were downloaded from the USGS Earth Explorer website. ERDAS Imagine software were used for processing of the imagery and image interpretation for the development of corresponding land use/land cover maps. The obtained maps are studied and analyzed to detect and compute the gradient.

Methodology/theory and calculations

Methodology included the wide spectrum of steps comprising thermal image processing (TIP) of archived Landsat data accessed from the Landsat Global Land Cover Facility (GLCF) website (<http://www.landcover.org>), weather data analysis of Climatological data—accessed from the (<http://www.mosdac.gov.in/>), land surface temperatures retrieval from TM band 6 (thermal infrared) by converting thermal brightness temperatures into thermodynamic (kinetic) temperatures and urban warming trend analysis by analyzing *LST* data over the entire regions (Li et al. 2012). The estimation of *LST* for SKT with only one thermal channel acted as the main advantage for single-channel methods (Alipour and Esmaeily 2005). Figure 2 describes the complete chain of operations required to retrieve the SKT image from the raw image acquired from Landsat Achieve. The figure also illustrates the complete process being performed to achieve the desired objectives.

Digital image processing

Digital image processing was manipulated by the software used. The scenes were selected to be geometrically corrected, calibrated, and removed from their dropouts. These data were stratified into ‘zones’, where land cover types within a zone have similar spectral properties. Other image enhancement techniques like histogram equalization are also performed on each image for improving the quality of

**Fig. 2** Flowchart of the complete sequence of work

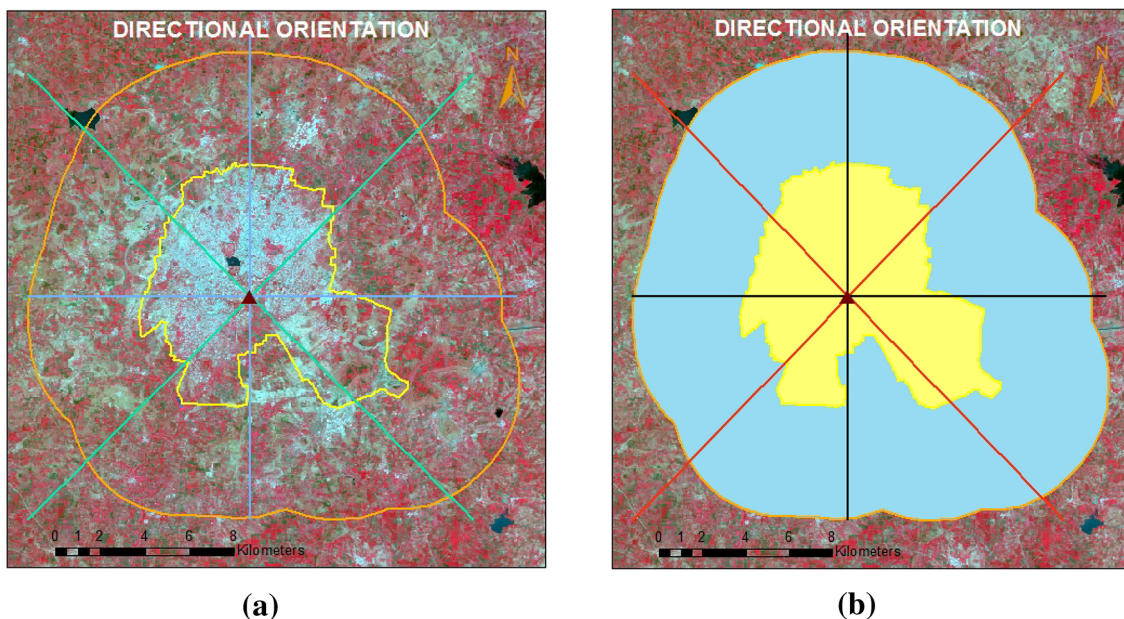


Fig. 3 Directional orientation for analysis. **a** Configuration for directional analysis. **b** Regions/extent of urban core and Rurban areas

the image. With the help of Survey of India topographic sheets of 1:50,000, the study area has been delineated. The data of ground truth were adapted for each single classifier produced by its spectral signatures.

Spatial variability analysis

Atmospheric forces and constituents have a strong impact on the solar radiation absorbed, reflected, or otherwise prevented from reaching the surface of the earth, and as the climate varies, so does the solar radiation available for a solar energy venture conceptualizes the focus of this paper. The characterization of the land surface temperature or surface KT is often not considered only in terms of magnitude but also in terms of how much surface temperature is available at an area of interest over a specific location. But a complete characterization includes the variability of available radiation can also consider the variability of the solar resource in space—how it varies over distance and spatial locations. Derived KT data were analyzed in the realms of spatial variability to derive the gradient. The analysis summarizes the geostatistical derived values in each orthogonal and cardinal directions namely North, South, East, West, North-East, South-East, South-West and North-West, respectively.

Ortho-directional trend patterns

The temperature transects values in each cardinal directions or zones along each direction with a spacing interval of 500 m distance from adjacent points to determine the

variability of the temperature within the surrounding, as depicted in Fig. 3.

Temperature gradient conceptualizations

A temperature gradient is a physical quantity describing direction and rate at which the temperature changes around a particular location. The temperature gradient is a dimensional quantity expressed in units of degrees (on a particular temperature scale) per unit length. Temperature gradients in the atmosphere are important in the atmospheric sciences (meteorology, climatology and related fields).The temp gradient is similar to finding the slope of a line (when in two dimensions) (Ottawa 1982). The SI unit is kelvin per meter (K/m).

$$dT/dx = (T2 - T1)/(X2 - X1) \tag{1}$$

In three dimensions, the temperature gradient is a vector found by taking the partial derivative of temperature with respect to x, y. Assuming that the temperature T is an intensive quantity, i.e., a single-valued, continuous and differentiable function of three-dimensional space (Ottawa 1982) (often called a scalar field), i.e., that

$$T = T(x, y) \tag{2}$$

where x, y are the coordinates of the location of interest, then the temperature gradient is the vector quantity defined as:

$$\nabla T = \left(\frac{\partial T}{\partial x}, \frac{\partial T}{\partial y}, \frac{\partial T}{\partial t} \right) \tag{3}$$

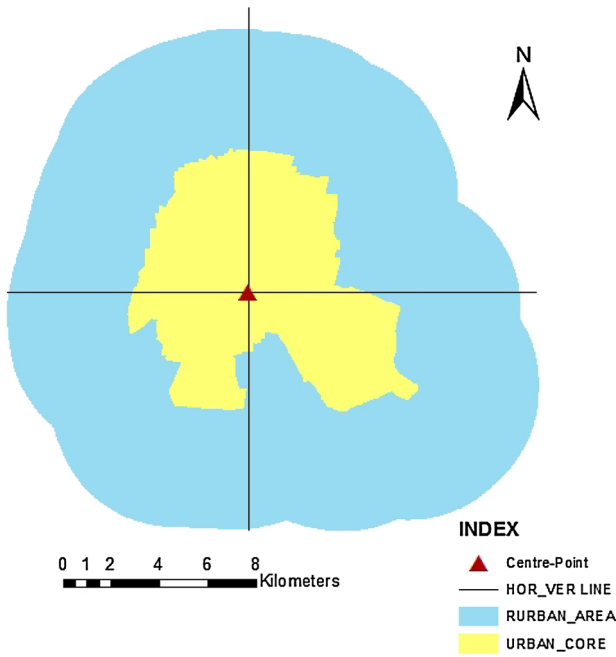


Fig. 4 Configuration of urban core and rural

In simple terms, the temperature gradient is defined as the change in temperature over the distance and expressed dT/dx . For Example, The temperature at point A is $10\text{ }^\circ\text{C}$, the temperature at point B is $20\text{ }^\circ\text{C}$, and point A is 100 km

from point B. The corresponding temperature gradient can be computed as (Fig. 4):

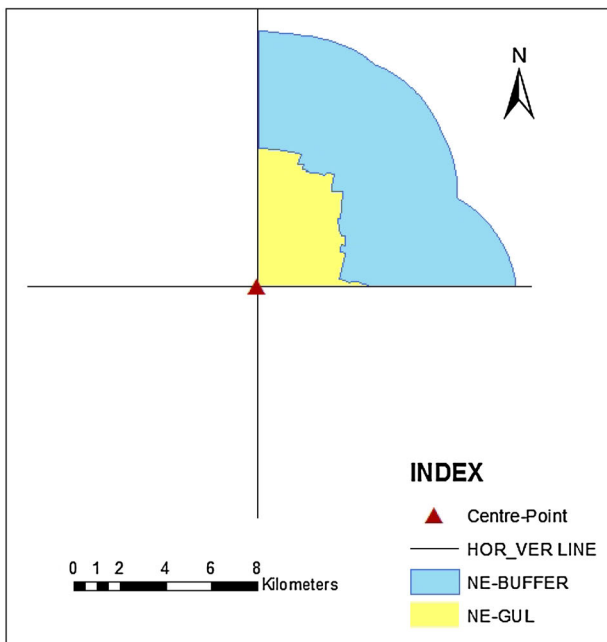
$$dT = 20\text{ }^\circ\text{C} - 10\text{ }^\circ\text{C} = 10\text{ }^\circ\text{C}, \quad dx = 100\text{ km};$$

$$dT/dx = 10\text{ }^\circ\text{C}/100\text{ km} = 0.1\text{ }^\circ\text{C}/\text{km}.$$

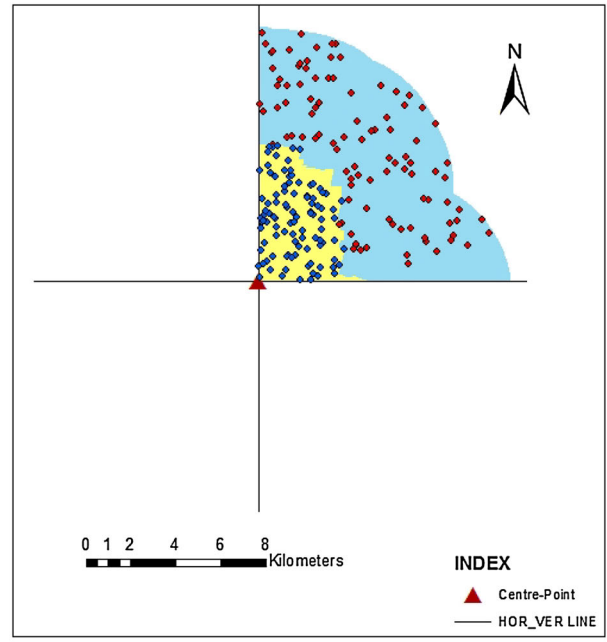
Spatial statistics (the correlogram)

Let $z(\mathbf{u}_\alpha)$, $\alpha = 1, 2, \dots, n$ denote the set of temperature values (n) measured using thermal remote sensing at the Core Urban and Rural area, where \mathbf{u}_α is the vector of spatial coordinates of the α th observation. Figure 5a, b shows the distributed temperature values along the North-East sector (with transect length of 12 km) at the Urban Core and Rural areas at randomly generated points. The similarity between adjacent temperature values can be depicted by plotting each observation $z(\mathbf{u}_\alpha)$ versus the one measured ‘ h ’ units away, $z(\mathbf{u}_\alpha + \mathbf{h})$ with ‘ h ’ normally varies between 0 and 100 m (maximum random points lies with radius of 100 m), 99 pairs of temperature estimations ($z(\mathbf{u}_\alpha)$, $z(\mathbf{u}_\alpha + \mathbf{h})$) are formed from the initial set of 100 values, and the resulting plot is called an h -scattergram (as shown in Fig. 5b; next page right top side diagram)

Similarly, distribution of temperature values for the urban core and Rural areas along the North-West, South-East and South-West direction was generated as fully random observations. The shape of the cloud of points on



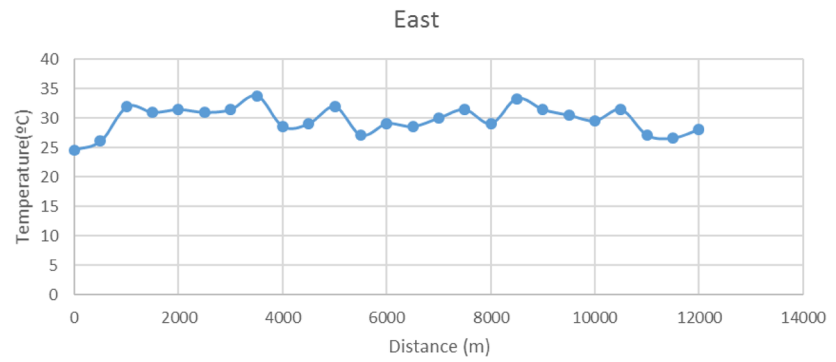
(a)



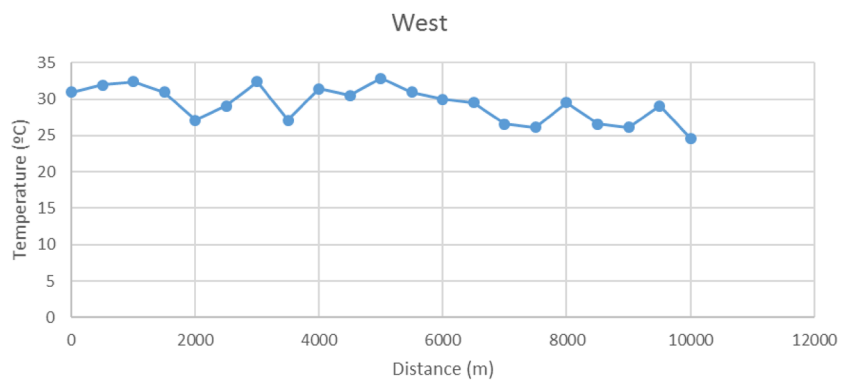
(b)

Fig. 5 a Configuration for Urban Core and Rural extent in North-East Lobe. b Point clouds in Urban and Rural extent in North-East Lobe

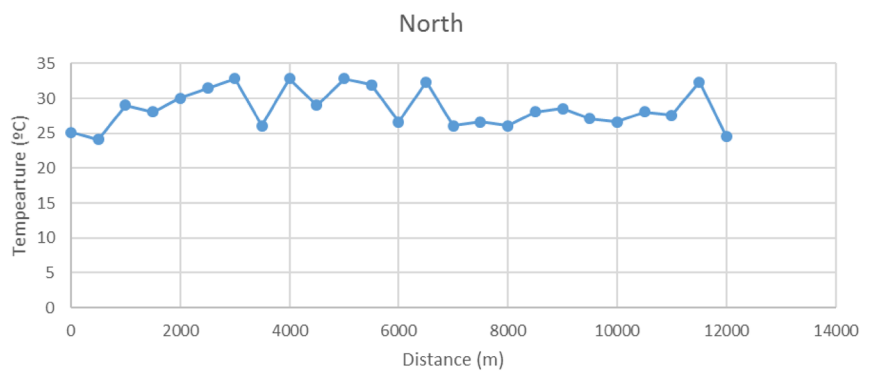
Fig. 6 Temperature transects in all directions. **a** Transects of temperature (East). **b** Transects of temperature (West). **c** Transects of temperature (North). **d** Transects of temperature (South)



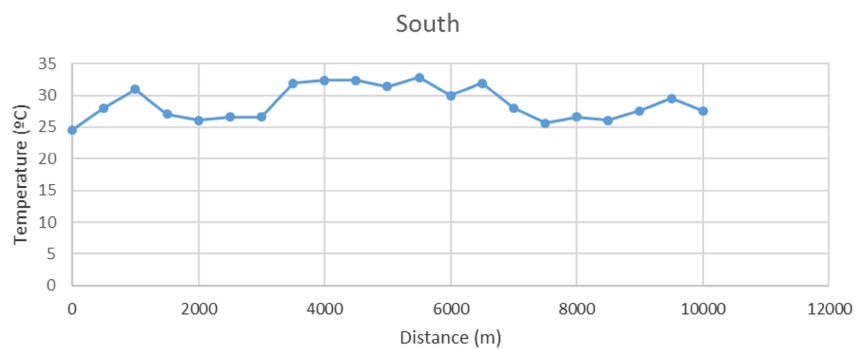
(a)



(b)



(c)



(d)

Table 2 Descriptive statistics for urban core vs. rurban areas

	Urban core-NE	Rurban-NE	Urban core-NW	Rurban-NW	Urban core-SE	Rurban-SE	Urban core-SW	Rurban-SW
Mean	28.650636	29.892360	28.206380	30.207098	29.102068	29.442052	29.960459	29.376960
Std. error of mean	0.2115727	0.1768306	0.2222166	0.2219448	0.2063857	0.1942597	0.2040123	0.2094262
Median	28.303328	30.475080	27.080935	30.475080	29.031509	29.514503	29.995691	29.514503
Mode	27.0809	30.9527	27.0809	31.4286 ^a	29.0315	29.5145 ^a	30.4751 ^a	30.4751
Std. deviation	2.1157269	1.7683057	2.2221659	2.2194482	2.0638567	1.9425967	2.0401227	2.0942624
Variance	4.476	3.127	4.938	4.926	4.260	3.774	4.162	4.386
Skewness	0.374	-0.472	0.664	-0.625	-0.004	-0.303	-0.201	-0.391
Std. error of skewness	0.241	0.241	0.241	0.241	0.241	0.241	0.241	0.241
Kurtosis	-0.606	-0.430	-0.290	0.392	-0.911	-0.312	-0.630	-0.202
Std. error of kurtosis	0.478	0.478	0.478	0.478	0.478	0.478	0.478	0.478
Range	10.1512	8.2154	10.1899	11.6264	8.2154	9.7225	8.2154	10.2291
Minimum	24.0968	25.0996	23.5924	23.0858	25.0996	23.5924	25.0996	23.0858
Maximum	34.2481	33.3149	33.7823	34.7122	33.3149	33.3149	33.3149	33.3149

^a Multiple modes exist. The smallest value is shown, number of random sample points = 10

the **h**-scattergram indicates that there is some correlation between adjacent temperature values, and this can be measured using the linear correlation coefficient which is traditionally used to assess the correlation between different attributes. The correlation values of 0.143 in The North-East direction agrees with our visual impression that the temperature value at any location in the urban core area is meagerly related to the temperature estimated in the rurban area. Intuitively, one would expect that the relation between temperature values weakens in the South-East direction, which is confirmed by the second **h**-scattergram the correlation drops from 0.143 to -0.109. The increasing inflation of the cloud of points reflects the decreasing similarity of measurements farther apart: the correlation at North-West and South-East is only 0.041 and 0.138 respectively.

The above Fig. 6 depicts the configuration for the spatial correlation analysis. The plot of the estimated correlation coefficients as a function of the separation distance is called the experimental correlogram (Goovaerts 1998). For the South-East direction, the correlation becomes negligible for Urban Core and Rurban Area at a separation distance of about 12 km radially outward from the center, which is referred to as the range and is interpreted at the distance beyond which two temperature values can be considered as statistically independent. The decline in correlation is much sharper in this lobe in two zones apart

can already be considered as independent. The correlogram thus allows one to quantify in terms of correlation the visual impression that small-scale fluctuations prevail for transects of North-West and South-West directions.

Results and discussions

Temperature transects trends descriptions

Figure 6a–d elucidates series of temperature values estimated at every half kilometer interval along East, West, North and South direction with 12 km stretch. The analysis of such data aggregates to plot the histogram to compute the summary statistics such as mean, median, mode, standard deviation, variance and skewness. The comparison of standard deviations are very much useful in predicting the variability of the temperature in different directions with similar types of distances. The spatial feature may be important for interpretation which is not captured if one ignores the spatial information. Geostatistics provides a set of statistical tools for detecting and quantifying the major scales of spatial variability (Tables 2).

Correlation values (urban vs. rurban)

See Table 3.

Table 3 Correlation table for urban core vs. rurban areas

	Urban core-NE	Rurban-NE	Urban core-NW	Rurban-NW	Urban core-SE	Rurban-SE	Urban core-SW	Rurban-SW
Urban core-NE								
Pearson correlation	1	0.143	0.132	-0.095	0.113	0.020	-0.126	0.049
Sig. (2-tailed)		0.154	0.191	0.345	0.262	0.842	0.213	0.628
N	100	100	100	100	100	100	100	100
Rurban-NE								
Pearson correlation	0.143	1	0.152	-0.174	0.040	-0.115	0.143	0.011
Sig. (2-tailed)	0.154		0.130	0.084	0.696	0.255	0.156	0.912
N	100	100	100	100	100	100	100	100
Urban core-NW								
Pearson correlation	0.132	0.152	1	0.041	0.070	-0.061	0.022	-0.019
Sig. (2-tailed)	0.191	0.130		0.685	0.488	0.548	0.826	0.852
N	100	100	100	100	100	100	100	100
Rurban-NW								
Pearson correlation	-0.095	-0.174	0.041	1	-0.056	0.134	0.004	0.110
Sig. (2-tailed)	0.345	0.084	0.685		0.581	0.184	0.968	0.277
N	100	100	100	100	100	100	100	100
Urban core-SE								
Pearson correlation	0.113	0.040	0.070	-0.056	1	-0.205*	-0.109	0.021
Sig. (2-tailed)	0.262	0.696	0.488	0.581		0.041	0.280	0.835
N	100	100	100	100	100	100	100	100
Rurban-SE								
Pearson correlation	0.020	-0.115	-0.061	0.134	-0.205*	1	0.111	0.196
Sig. (2-tailed)	0.842	0.255	0.548	0.184	0.041		0.270	0.051
N	100	100	100	100	100	100	100	100
Urban core-SW								
Pearson correlation	-0.126	0.143	0.022	0.004	-0.109	0.111	1	0.138
Sig. (2-tailed)	0.213	0.156	0.826	0.968	0.280	0.270		0.171
N	100	100	100	100	100	100	100	100
Rurban-SW								
Pearson correlation	0.049	0.011	-0.019	0.110	0.021	0.196	0.138	1
Sig. (2-tailed)	0.628	0.912	0.852	0.277	0.835	0.051	0.171	
N	100	100	100	100	100	100	100	100

* Correlation is significant at the 0.05 level (2-tailed). Number of random points = 100

Descriptive statistics (urban vs. rurban)

See Table 4.

Table 4 Urban core vs. rurban in North-East direction

	Urban core values (°C)	Rurban values (°C)
Mean	28.650636	29.892360
Std. error of mean	0.2115727	0.1768306
Median	28.303328	30.475080
Mode	27.0809	30.9527
Std. deviation	2.1157269	1.7683057
Variance	4.476	3.127

Table 4 continued

	Urban core values (°C)	Rurban values (°C)
Skewness	0.374	-0.472
Std. error of skewness	0.241	0.241
Range	10.1512	8.2154
Minimum	24.0968	25.0996
Maximum	34.2481	33.3149

Table 5 Comparative table showing gradient values in all directions

Sl. No	Direction	Linear curve equation	R ² values	Slope values (<i>p</i>)
1.	North	$y = -8E-05x + 29.023$	0.0105	-0.00008
2.	South	$y = 2E-05x + 28.642$	0.0007	-0.00002
3.	East	$y = -2E-05x + 29.848$	0.0008	-0.00002
4.	West	$y = -0.0005x + 31.756$	0.3836	-0.0005
5.	North-East	$y = 0.0002x + 27.48$	0.2414	-0.0002
6.	South-East	$y = -0.0001x + 30.138$	0.0737	-0.0001
7.	South-West	$y = -6E-05x + 29.359$	0.021	-0.00006
8.	North-West	$y = 1E-04x + 27.918$	0.0156	-0.0001

Interpretation and analysis

The data present in Table 4 describes the comparative values between urban core vs. rurban through different statistical parametric values. The spatial variability of the thermal gradient in all ortho-directions results produces the spatial metrics and indices to quantify the amount of variability in diverse dimensions. Accumulation of surface temperature datasets availability for future use by managers, planners, public health officials, ecologists, and researchers. The other part of study comprises the calculation of intensity or magnitude of the thermal gradient in all directions. The complexity in trend pattern of UHI due to increasing growth from urban center to adjoining non-build-up areas in all directions. An estimated temperature range for the surface in degree celsius (mostly for roof tops and for the vegetation). The gradient curves for all the directions were being plotted and reported in tabular format with linear curve equations. The outcomes are obtained from the geostatistical analysis of LST gradient variance in rural-urban scenario (i.e. in built-up area vs. rural) were also report.

Table 5 Signifies that gradient/slope value very non-significant in almost all the directions. It reveals the fact that the slope is negative in everywhere, which implies that there are negative trends of the temperature gradient with respect to distance. In particular, the South and East directions reflects the similar type of temperature gradient. Similarly, the South-East and North-West shows similar

trends of the gradient values. Which means that there is a decrease in temperature by a factor of *p* times of each 500 or 707 m of distance. The West and Northeast directions indicate the maximum values of rate of variations. The central part demonstrates urban growth resulting maturation of vegetation decline. Additional analysis of surface temperatures for established urban development areas within city vs. newly developed areas will permit analysis of the degree to which outdoor urban temperatures declines. The study identified the packets in study area having higher global solar radiation contributing to heat islands. Beyond these, the study provided surface temperature gradient on spatial scale correlated to urban growth, including zonal gradient analysis. The outcome obtained from the geostatistical analysis of land surface temperature also summarizes the leading temperature variations in Urban Core area vs. Rurban areas. This also illustrated the complexity in trend pattern of temperature due to increasing growth from urban center to adjoining rurban non-build-up areas in all cardinal directions. Estimated temperature ranges from 20.52 to 35.64 °C for the surface in degree celsius (mostly for roof tops and for the vegetation) in the study area.

Spatial distribution characteristics

These maps indicated that a wide range of variability exists in the surface radiance temperature, and the values range from insignificant (in the context of measurements and

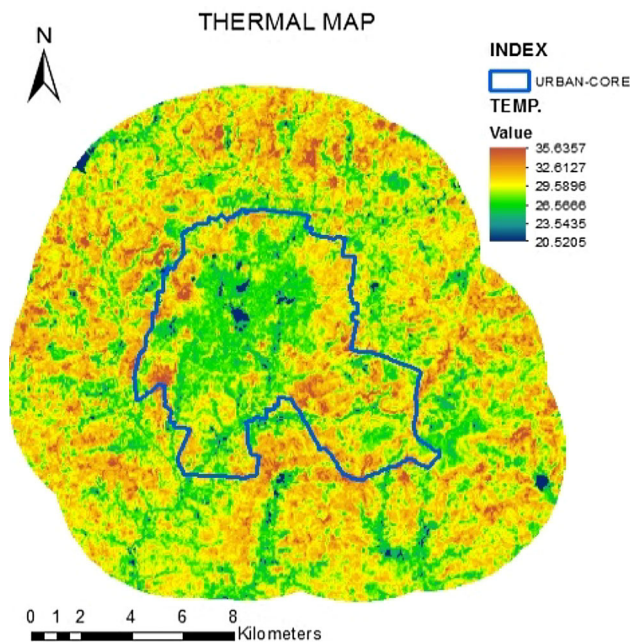


Fig. 7 Temperature distribution map

economic analyses) to highly significant. Consequently, the uncertainty of this analysis has not been defined.

Geostatistical characteristics

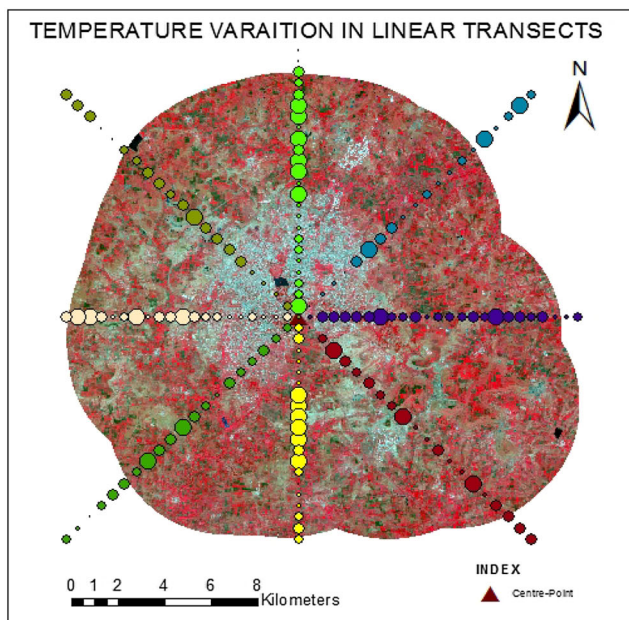
Visual interpretation of the surface temperature in Fig. 7 gives the contrast of temperature variation. Furthermore,

any quantitative processing of temperature information is incomplete as long as it takes no account of the spatial coordinates of observations. Geostatistical characterization of the spatial variability through semivariogram or correlograms generally brings new insight into the way temperature attributes are influenced by the environment, such as geographical distribution of or topography.

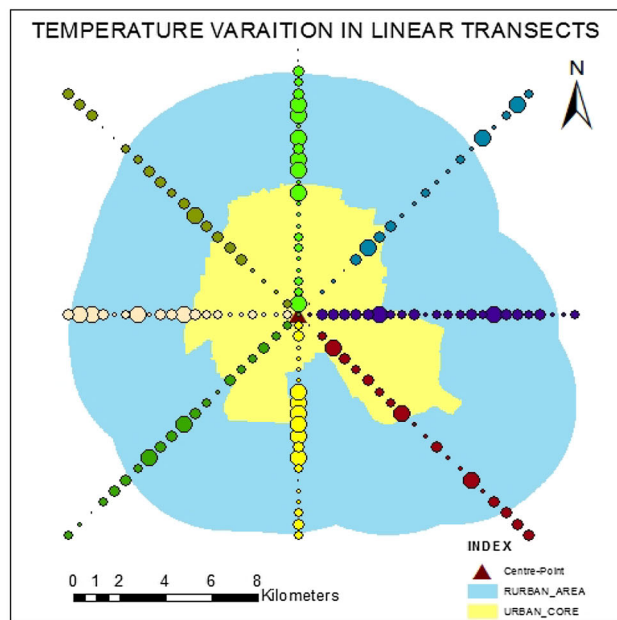
Discussions

Linear transects in Fig. 8a, b infers that there is very little variations of temperature in the urban core areas due to the homogeneity of the land use and land cover, whereas the fluctuations can be easily observed near the periphery of the urban core areas. These fluctuations are also due to the movement of hot air to cold regions. In almost all the sectors the fluctuations are perpetual, which can be easily interpreted by the graduated mapping symbology used to represent the values of temperatures at each 500 m in North, East, West and South directions and 707 m interval in North-East, North-West, South-East and South-West direction.

Similarly, Figs. 9a–d gives the inferences for the interpretation of correlation in each lobe (viz. North-East, South-East, South-West, and North-West) between the urban core and rurban areas. Table 4 also confirms that the North-East sector of Rurban areas shows the least standard mean error with the values of 0.1768306 and the North-



(a)



(b)

Fig. 8 a Temperature variation transects in study area. b Temperature variation transects overlaid in Urban core and Rurban area

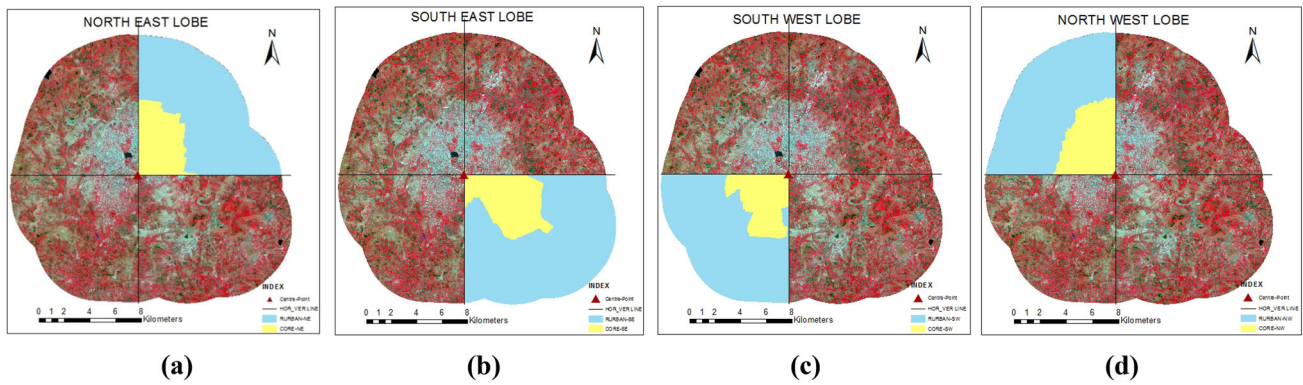
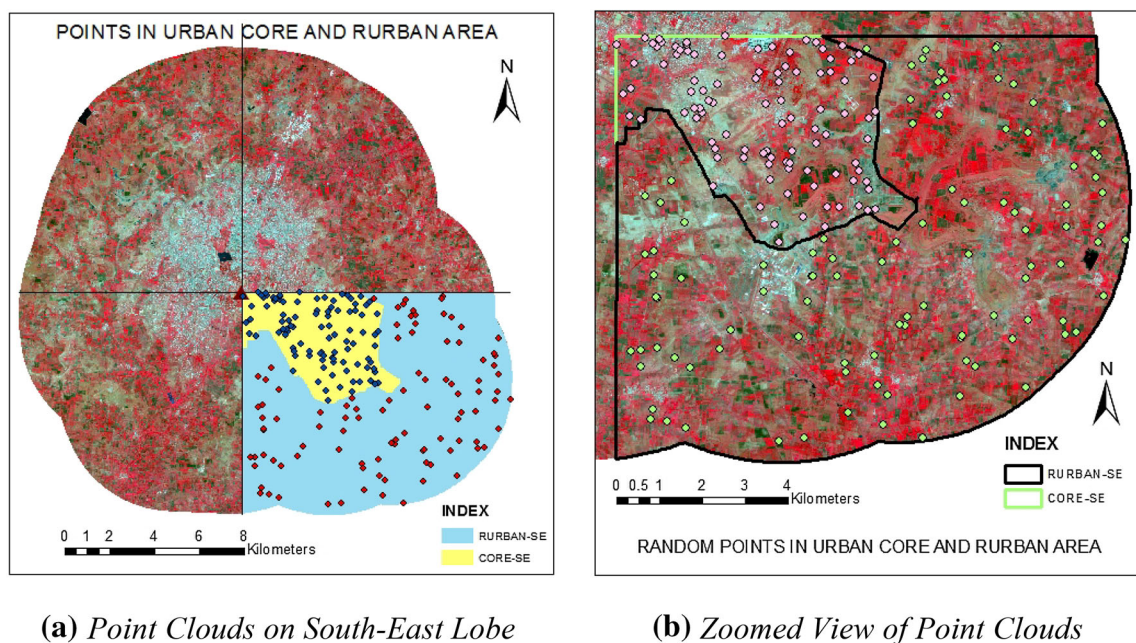


Fig. 9 Urban core and Rurban area configuration in North-East lobe (a), South-East lobe (b), South-West lobe (c) and North-West lobe (d)



(a) Point Clouds on South-East Lobe

(b) Zoomed View of Point Clouds

Fig. 10 Illustration for detailed study of South-East lobe

West lobe contains the highest standard mean error with the values of 0.2222166. Apart from these North-West rurban and South East rurban contains the multiple modes with the values of 31.4286 and 29.5145 respectively.

Table 3 shows the inter-correlation of core urban area and rurban area in different sectorial lobes, if we consider the case of the North-East lobes along with randomly generated point’s clouds for the urban core areas as well as Rurban, we observe that the significant amount of correlation exists between them with a correlation coefficient of 0.143. Similarly considering the North-West lobe we got a correlation coefficient of 0.041, in the South-West lobe we get the correlation coefficient of 0.138 but when we see the case of South-East Lobes, it gives us the slightly different

characteristics results with a correlation coefficient of negative values with -0.109 . Which also infers that the temperature values of Core-Urban and Rurban areas in this lobes are significantly uncorrelated from each other. Which gives us the opportunity to explore this region furthermore in details.

Illustrative case study: interpretation of South-East lobe

Figure 10a shows the location of The South-East lobe along with the randomly generated point clouds in core urban (shown in yellow color) and rurban area (shown in light blue color).When we zoom into the land use and land

cover of the area then it is very easy to derive the inference information about the mystery behind the negative correlation values in this lobes. If we see the urban core area in this lobe then we observe that almost 60–70 percent of the area is being covered by built-up land which may cause the increase in the nearby by areas but when we see the rural extent of the same lobe then it can be seen that majority of the land cover is empty of being covered by the vegetation, which may cause the drop in temperature values resulting in the moderate temperature. So these collective set of high and low-temperature ranges are when being correlated together results in the negative correlation values. Figure 10b visualizes the orientation of the points at a closer level.

Conclusions

The current work proposes to formulate the methods focused on extraction techniques of quantitative information from thermal data with reasonable aspects of thermal image processing (TIP) of archived Landsat data for characterization of spatial (x, y) and temperature/thermal (t) trends. The work utilized the procedures ranging from detect the extent of urban and rural extent detection, computing at-surface kinetic temperature, allocating the obtained result into sectors or ortho-directions, visualizing the boundary of the urban core limits and its rural extents, generating random sample points for each of the sectoral limits of urban core as well as in rural extent, analyzing the degree of similarity vs dissimilarity, investigating the structure and patterns of variability, examining the urbanization impact on the land cover/land use changes, and computing the gradient along the ortho-directional sectors.

The variability measurements indicated that the spatial distribution of vegetation is opposite to that of higher at-surface kinetic temperature and also revealed that urban at-surface kinetic temperature and also has a close relation to the abundance of vegetation cover. The temperature transects along each cardinal directions or zones (i.e. North, East, South and West) with a spacing of 500 m showed the complex trends of variation and also illuminated the ambiguities behind it. Similarly, the temperature gradient, on the contrary, conceptualized about the rate of urbanization due to the increasing gradient values from Urban to Rural areas. The work also inferred that the consistency of at-surface kinetic temperature may act as an indicator to depict the potential solar resource zones with having greater solar radiations. Beyond these, the study delivered thermal gradient on spatial scale correlated to urban growth for presenting the zonal gradient analysis. For validation of results, efforts were taken to collect the weather data measured by India Meteorological Department (an agency

of the Ministry of Earth Sciences of the Government of India), which will further enhance the results. These complex problem needs to be seriously studied, through multi-dimensional fields in order to enhance the precious and limited knowledge base about gradient analysis.

Compliance with ethical standards

Conflict of interest The authors declare that there is no conflict of interests regarding the publication of this paper.

References

- Alipour T, Esmaeily A (2005) Land surface temperature estimation from thermal band of landsat sensor, case study: Alashtar city (2003)
- Bayat B, Zahraie B, Taghavi F, Nasseri M (2012) Evaluation of spatial and spatiotemporal estimation methods in simulation of precipitation variability patterns. *Theoret Appl Climatol* 113(3–4):429–444. doi:10.1007/s00704-012-0795-7
- Belal AA, Moghanm F (2011) Detecting urban growth using remote sensing and GIS techniques in Al Gharbiya governorate, Egypt. *Egypt J Remote Sens Space Sci* 14(2):73–79. doi:10.1016/j.ejrs.2011.09.001
- Demeritt D, Wainwright J (2005) Models, modelling, and geography
- Florinsky IV, Kulagina TB, Meshalkina JL (1994) Influence of topography on landscape radiation temperature distribution. *Remote Sens* 15(1):1–7
- Goovaerts P (1998) Geostatistical tools for characterizing the spatial variability of microbiological and physicochemical soil properties. *Biol Fertil Soils* 27(4):315–334. doi:10.1007/s003740050439
- Iqbal MF, Khan IA (2014) Spatiotemporal Land Use Land Cover change analysis and erosion risk mapping of Azad Jammu and Kashmir, Pakistan. *Egypt J Remote Sens Space Sci* 17(2):209–229. doi:10.1016/j.ejrs.2014.09.004
- Jones HG, Schofield P (2008) Thermal and another remote sensing of plant stress. *General Appl Plant Physiol* 34:19–32. http://www.bio21.bas.bg/ipp/gapbfiles/v-34_pisa-08/08_pisa_1-2_19-32.pdf
- Kanyakumari LN, Neelamsetti P (2015) Multi-temporal land use classification using a hybrid approach. *Egypt J Remote Sens Space Sci*. doi:10.1016/j.ejrs.2015.09.003
- Li Y, Zhang H, Kainz W (2012) Monitoring patterns of urban heat islands of the fast-growing Shanghai metropolis, China: using time-series of Landsat TM/ETM + data. *Int J Appl Earth Obs Geoinformation* 19:127–138
- Ottawa C (1982) Estimating temperature gradients and dew point temperatures (March)
- Panhalkar SS (2014) Hydrological modeling using SWAT model and geoinformatics techniques. *Egypt J Remote Sensing Space Sci* 17(2):197–207. doi:10.1016/j.ejrs.2014.03.001
- Rawat JS, Kumar M (2015) Monitoring land use/cover change using remote sensing and GIS techniques: a case study of Hawalbagh block, district Almora, Uttarakhand, India. *Egypt J Remote Sens Space Sci* 18(1):77–84. doi:10.1016/j.ejrs.2015.02.002
- Shao J, Swanson JC, Patterson R, Lister PJ, McDonald AN (1997) Variation of winter road surface temperature due to topography and application of Thermal Mapping. *Meteorol Appl* 4(2):131–137. doi:10.1017/S135048279700042X
- Sinha S, Sharma LK, Nathawat MS (2015) Improved land-use/land-cover classification of semi-arid deciduous forest landscape using thermal remote sensing. *Egypt J Remote Sens Space Sci*. doi:10.1016/j.ejrs.2015.09.005

- Stein A, Zinck JA (1998) Spatial variability of soil properties at different scales within three terraces of the Henares River, Spain
- Sun L, Fukuda T, Tokuhara T, Yabuki N (2014) Differences in spatial understanding between physical and virtual models. *Frontiers Archit Res* 3(1):28–35. doi:[10.1016/j.foar.2013.11.005](https://doi.org/10.1016/j.foar.2013.11.005)
- Wei MA, Yun-hao C, Ji Z (2008) Quantitative analysis of land surface temperature-vegetation indexes relationship based on remote sensing. *Int Arch Photogramm Remote Sens Spatial Inf Sci XXXVII(Part B 6b)*:261–264
- Yuan F, Bauer ME (2007) Comparison of impervious surface area and normalized difference vegetation index as indicators of surface urban heat island effects in Landsat imagery. *Remote Sens Environ* 106(3):375–386. doi:[10.1016/j.rse.2006.09.003](https://doi.org/10.1016/j.rse.2006.09.003)